Synthesis, biological evaluation, and docking studies of gigantol analogs as calmodulin inhibitors

By: Adelfo Reyes Ramírez, Martha Leyte-Lugo, Mario Figueroa, Trinidad Serrano-Alba, Martín González, and Rachel Mata

Reyes-Ramírez, A., Leyte-Lugo, M., Figueroa, M., Serrano-Alba, T., González-Andrade, M., Mata, R. (2011). Synthesis, biological evaluation, and docking studies of gigantol analogs as calmodulin inhibitors. *European Journal of Medicinal Chemistry, 46* (7), pp. 2699-2708. DOI: 10.1016/j.ejmech.2011.03.057

Abstract:

Several analogs of gigantol (**1**) were synthesized to evaluate their effect on the complexes Ca^{2+}–calmodulin (CaM) and Ca^{2+}–CaM–CaM sensitive phosphodiesterase 1 (PDE1). The compounds belong to four structural groups including, 1,2-diphenylethanes (**2**–**11**), diphenylmethanes (**13**–**15**), 1,3-diphenylpropenones (**16**–**18**), and 1,3-diphenylpropanes (**20**–**22**). *In vitro* enzymatic studies showed that all compounds except **11** inhibited the complex Ca^{2+}–CaM–PDE1 with IC_{50} values ranging from 9 to 146 μM. On the other hand, all analogs but **11**, **12** and **15** quenched the extrinsic fluorescence of the CaM biosensor *h*CaM–M124C–*mBBr* to different extent, then revealing different affinities to CaM; their affinity constants (K_m) values were in the range of 3–80 μM. Molecular modeling studies indicated that all these compounds bound to CaM at the same site that the classical inhibitors trifluoperazine (TFP) and chlorpromazine (CPZ). Some of these analogs could be worthy candidates for developing new anti-tumor, local anesthetics, antidepressants, antipsychotic, or smooth muscle relaxant drugs, with anti-CaM properties due to their good affinity to CaM and the straightforwardness of their synthesis. In addition they could be valuable tools for the study of Ca^{2+}–CaM functions.

Graphical abstract: Some synthetic 1,2-diphenylethanes, diphenylmethanes, 1,3-diphenylpropenones, and 1,3-diphenylpropanes inhibited Ca^{2+}–CaM–PDE1 complex and quenched the fluorescence of *h*CaM–M124C–*mBBr*.

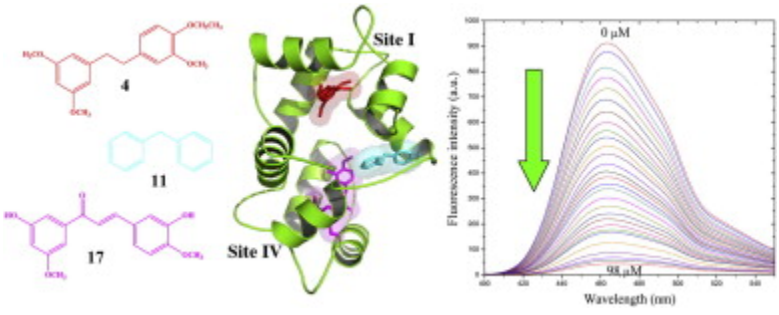

Keywords: 1,2-Diphenylethanes | 1,3-Diphenylpropenones | 1,3-Diphenylpropanes | Calmodulin | Gigantol

Article:

1. Introduction

Gigantol (**1**) is a naturally occurring 1,2-diphenylethane (bibenzyl) isolated from several medicinal orchids. In previous investigations, the anti-inflammatory, antinociceptive, phytotoxic, and spasmolytic properties of **1** and a few synthetic 1,2-diphenylethanes were demonstrated [1], [2], [3], [4], [5]. It was also found that for maximum spasmolytic activity, these products should have oxygenated substituents on both aromatic rings [5]. The spasmolytic 1,2-diphenylethanes or bibenzyls also inhibited the complex Ca^{2+}–calmodulin (CaM)–CaM-sensitive phosphodiesterase 1 (PDE1) and potentiated the antispasmodic action of chlorpromazine (CPZ), a classical CaM inhibitor [5]. Altogether, these results suggested that these compounds were CaM inhibitors and that their smooth muscle relaxant activity was mediated by CaM [1], [5].

CaM is a major cellular Ca^{2+}–binding protein, which is ubiquitously expressed in all the eukaryotic cells [6]. This protein does not possess enzymatic activity, however modulates several enzymes and ion channels involved in a variety of physiological events including regulation of metabolism, cytoskeleton, ion transport, protein folding, cell proliferation, cell division as well as protein phosphorylation and dephosphorylation, among others. Therefore, Ca^{2+}–CaM and Ca^{2+}–CaM-protein complexes are of significant biomedical interest as molecular targets for the development of new drugs useful for treating pathological processes related with CaM [7]. Indeed, CaM-induced target enzyme activation can be blocked by several classes of pharmacological effectors: antipsychotics, antidepressants, muscle relaxants, and local anesthetics.

In this study we describe the synthesis and the anti-CaM effect (*in vitro* and *in silico*) of twenty compounds (**2**–**22**) structurally related to gigantol (**1**), which on the basis of the above considerations could be a suitable lead for the discovery of new CaM antagonists. As compound **1**, analogs **2**–**11** contain an ethylene bridge and two aromatic rings, with oxygenated or nitrogenated substituents of diverse polarity in different positions; these modifications would be useful for ascertaining the influence of the nature and location of the substituents along the 1,2-diphenylethane core on the anti-CaM effect of gigantol (**1**). Compound **12**, includes a heteroatom in the bridge and possesses no subtituents at the aromatic rings. On the other hand, to assess the contribution of the size and nature of the carbon chain between the two phenyls, analogs **13**–**22** were also analyzed. Analogs **13**–**15** are diphenylmethanes, **16**–**18** 1,3-diphenylpropenones (chalcones), and **20**–**22** are 1,3-diphenylpropanes. Thus, the last three set of compounds differ in the number of carbon atoms linking the two aromatic rings and their degree of oxidation. It is important to point out that diphenylmethanes, 1,3-diphenylpropanes or the chalcones have not previously tested as anti-CaM agents therefore the corresponding scaffold could be a new leads for the development of new CaM antagonists.

2. Results and discussion

Compounds **1**–**10** were obtained using the Wittig reaction, a method widely used for the synthesis of 1,2-diphenylethanes [5]. In all cases, the phosphonium salts were prepared by the reaction of triphenylphosphine with an appropriated alkyl halide; the resulting salts were dissolved in THF and deprotonated with NaH to yield a mixture of *Z*- and *E*-stilbenes, which were reduced by treatment with catalytic amounts of 10% Pd–C over H_2 (4 atm) to afford the 1,2-diphenylethanes [5]; the general route employed is summarized in Scheme 1. The yields ranged from 41 to 72%. Compounds **4**–**7**, **9**, and **10** are new chemical entities, while **3** was isolated from a *Dendrobium* species [8]. Finally, bibenzyls **2** and **8** were previously synthesized [9]. Diphenylmethanes **13** and **14** were obtained by an acid catalyzed intramolecular rearrangement of benzyl phenyl ether **26** (Scheme 2), which in turn was prepared by an *O*-alkylation of guaiacol with 3,5-dimethoxybenzyl bromide (**25**) in basic conditions [10]. Chalcones **16**–**19** were synthesized via a base catalyzed aldol condensation of the appropriate acetophenone (**27a**–**27c**) with a suitable benzaldehyde derivative (**24b**, **24c** and **24g**–**24h**). Finally, 1,3-diphenylpropanes **20**–**22** were obtained by one-step catalytic reduction of chalcones **16** [11], **18**, and **19** using H_2SO_4 and 10% Pd/C, in ethanol at 60 °C (Scheme 3). Compounds **17**–**22** are reported by the first time. The structures of synthetic analogs **1**–**11**, **13**, **14**, and **17**–**22** were elucidated on the basis of 1D-, 2D-NMR, and MS studies.

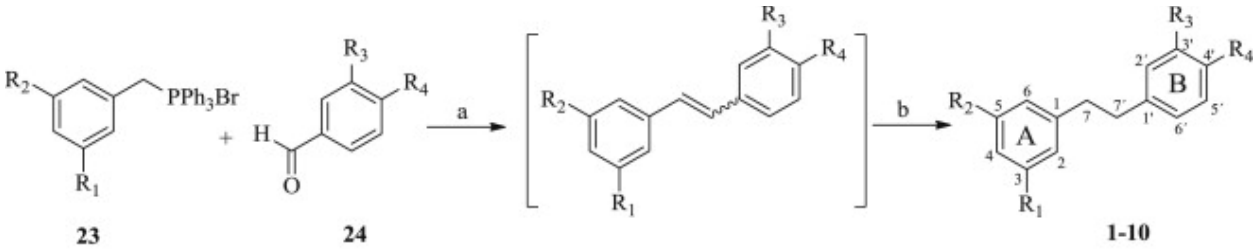

23a	R_1=OCH_2Ph, R_2=OCH_3	**24a**	R_3=OCH_3, R_4=OCH_2Ph	**1**	R_1=R_4=OH, R_2=R_3=OCH_3
23b	R_1=OH, R_2=H	**24b**	R_3=H, R_4=OCH_3	**2**	R_1=OH, R_2=R_4=OCH_3, R_3=H
23c	R_1=R_2=OCH_3	**24c**	R_3=R_4=OCH_2O	**3**	R_1=OH, R_2=OCH_3, R_3, R_4=OCH_2O
		24d	R_3=OCH_3, R_4=OCH_2CH_3	**4**	R_1=R_2=R_3=OCH_3, R_4=OCH_2CH_3
		24e	R_3=H, R_4=$N(CH_3)_2$	**5**	R_1=OH, R_2=OCH_3, R_3=H, R_4=$N(CH_3)_2$
				6	R_1=R_2=OCH_3, R_3=H, R_4=$N(CH_3)_2$
				7	R_1=OH, R_2=H, R_3, R_4=OCH_2O
				8	R_1=R_2=R_4=OCH_3, R_3=H
				9	R_1=OH, R_2=H, R_3=OCH_3, R_4=OCH_2CH_3
				10	R_1=OH, R_2=R_3=OCH_3, R_4=OCH_2CH_3

Scheme 1. Reagents and conditions for the synthesis of 1,2-diphenylethanes **1**–**10**: (a) NaH, THF; (b) H_2, 10% Pd–C, EtOAc.

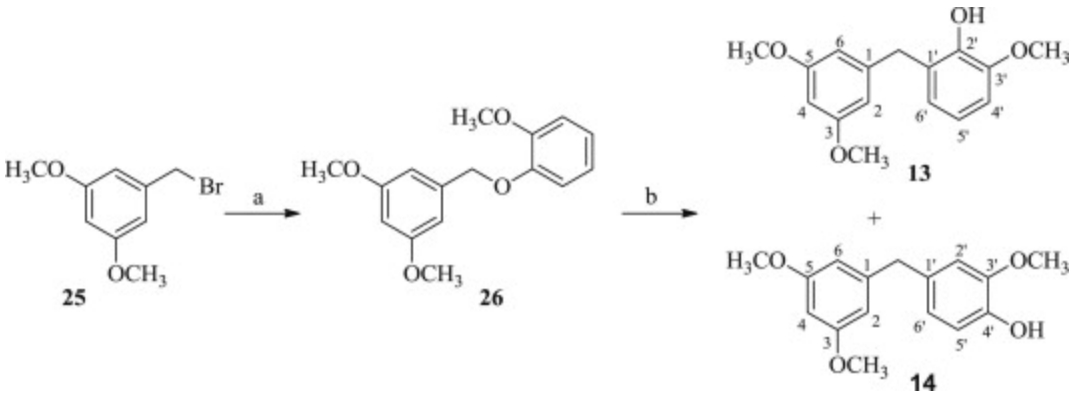

Scheme 2. Reagents and conditions for the synthesis of compounds **13** and **14**: (a) guaiacol, K_2CO_3, acetone; (b) H_3PO_4, toluene.

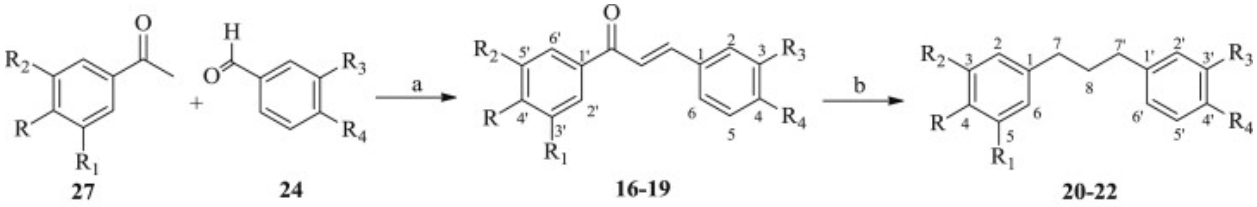

27a	R=OH, R_1=R_2=H	**24b**	R_3=H, R_4=OCH_3	**16**	R=OH, R_1=R_2=R_3=H, R_4=OCH_3
27b	R=H, R_1=OCH_3, R_2=OH	**24c**	R_3=R_4=OCH_2O	**17**	R=H, R_1=R_4=OCH_3, R_2=R_3=OH
27c	R=R_2=H, R_1=OH	**24f**	R_3=OH, R_4=OCH_3	**18**	R=H, R_1=R_3=OCH_3, R_2=R_4=OH
		24g	R_3=OCH_3, R_4=OH	**19**	R=R_2=H, R_1=OH, R_3, R_4=OCH_2O
				20	R=OH, R_1=R_2=R_3=H, R_4=OCH_3
				21	R=R_2=H, R_1=OH, R_3, R_4=OCH_2O
				22	R=H, R_1=R_3= OCH_3, R_2=R_4=OH

Scheme 3. Reagents and conditions for the synthesis of 1,3-diphenylpropenones **16**–**19** and 1,3-diphenylpropanes **20**–**22**: (a) KOH, EtOH; (b) Pd–C 10%, EtOH–H_2SO_4.

The *in vitro* anti-CaM activity of compounds **1**–**18** and **20**–**22** was determined using two methodologies; the first one, enzymatic in nature, employed PDE1 as monitoring enzyme and, assesses the action of the test compounds on the complex Ca^{2+}–CaM–PDE1 [12], [13]. The second analysis measures the direct interaction and affinity of any compound to the complex Ca^{2+}–CaM; for this assay a *h*CaM M124C–*mBBr* fluorescent biosensor was used [14]. The results (Table 1 and Fig. 1) showed that all compounds but **11**, **12**, and **15** did not bind to the complex Ca^{+2}–CaM. These three compounds have in common the absence of substituents in rings A and B of the 1,2-diphenylethane, diphenylmethane or benzylphenoxy cores (see Scheme 1) suggesting that the substitution at both aromatic rings, regardless of the nature and number of the bridge carbons, is an important structural feature for Ca^{+2}–CaM binding. This assumption was further confirmed throughout the docking analysis (*vide* infra, Table 1). In any case, however, the position of the phenols did not have a clear impact on the affinity to the protein.

Regarding their effect on the complex Ca^{2+}–CaM–PDE1, **11** and **12** did not inhibit the hydrolysis of *c*AMP; however **15** clearly displayed an inhibitory effect of the enzymatic activity with an IC_{50} of 15 μM. The latter results suggested that **15** could be affecting any components enzymatic assay including the snake nucleotidase or the PDE1. These results

showed the pitfalls of the enzymatic assay and the robustness of direct measurements using a *h*CaM M124C–*mBBr* fluorescent biosensor.

Table 1. Activity on the Ca^{+2}–CaM–PDE1 and properties of binding on the Ca^{+2}–CaM complex of compounds **1**–**22**.

Compound	Enzymatic PDE1 assay	Fluorescence quenching	
	IC_{50} (μM)[a]	K_m (μM)[b]	*h*[c]
CPZ	10.3 ± 1.02	5.55 ± 0.09	1.28 ± 0.02
1	114.18 ± 6.17	60.82 ± 4.12	1.23 ± 0.04
2	9.38 ± 2.48	80.04 ± 6.17	0.96 ± 0.05
3	31.29 ± 5.12	45.48 ± 1.98	1.59 ± 0.06
4	18.44 ± 6.53	9.88 ± 0.40	2.01 ± 0.12
5	30.10 ± 2.90	12.03 ± 0.38	1.55 ± 0.05
6	36.33 ± 7.39	10.00 ± 0.19	2.55 ± 0.12
7	75.89 ± 9.02	63.77 ± 2.86	1.52 ± 0.06
8	146.35 ± 32.46	21.82 ± 1.32	2.12 ± 0.14
9	46.09 ± 4.01	58.08 ± 5.11	1.26 ± 0.13
10	54.69 ± 6.22	25.26 ± 1.58	1.88 ± 0.20
11	NI	NB	NB
12	NI	NB	NB
13	56.15 ± 14.89	33.79 ± 5.06	1.01 ± 0.06
14	54.73 ± 6.47	33.07 ± 4.58	1.00 ± 0.06
15	15.02 ± 4.19	NB	NB
16	22.53 ± 6.52	10.27 ± 0.70	1.82 ± 0.17
17	37.68 ± 6.81	3.89 ± 0.05	1.72 ± 0.03
18	57.27 ± 15.21	5.31 ± 0.21	1.49 ± 0.05
20	62.68 ± 3.59	8.70 ± 0.15	1.35 ± 0.03
21	22.94 ± 4.05	14.21 ± 0.85	0.90 ± 0.03
22	32.54 ± 6.06	54.33 ± 6.41	0.97 ± 0.06

NB = not bind.
NI = not inhibit.
[a] Concentration inhibiting by 50% the activity of the enzyme.
[b] Apparent constant.
[c] Hill coefficient.

The remaining analogs tested showed different affinities to the protein with K_m values in the range of 3–80 μM. On the other hand, compounds **11**, **12** and **8** did not affect the complex Ca^{+2}–CaM–PDE1; the other compounds (**1–7**, **9**, **10**, **13–18**, **20–22**) however, inhibited the activation of PDE1 with IC_{50} values ranging from 9 to 75 μM.

Among the group of 1,2-diphenylethanes, compounds **4–6** exhibited the highest affinity to the protein with K_m of 9, 12 and 10 μM, respectively. The better affinity of compound **5** in comparison to **1** revealed that the presence of a tertiary amine in ring B increased the affinity to the protein by five times. On the other hand, comparison of the K_m values of **1** and **10** (K_m of 60 and 25 μM, respectively), clearly indicated that the etherification of the free phenol group at C-4 in ring B improved the affinity for the protein almost three fold. The lower K_m value for compound **4** (K_m = 9.88 μM), in comparison with **10** (K_m = 25.26 μM) further supports this comportment. Comparison of the K_m values of compounds **4**, **10**, and **9** (9, 25, and 58 μM, respectively) with those of **2**, **3**, **7**,and **8** (K_m of 80, 45, 63, and 21 μM, respectively), strengthened the relevance of hydrophobic substituents for better affinity to Ca^{+2}–CaM *in vitro*.

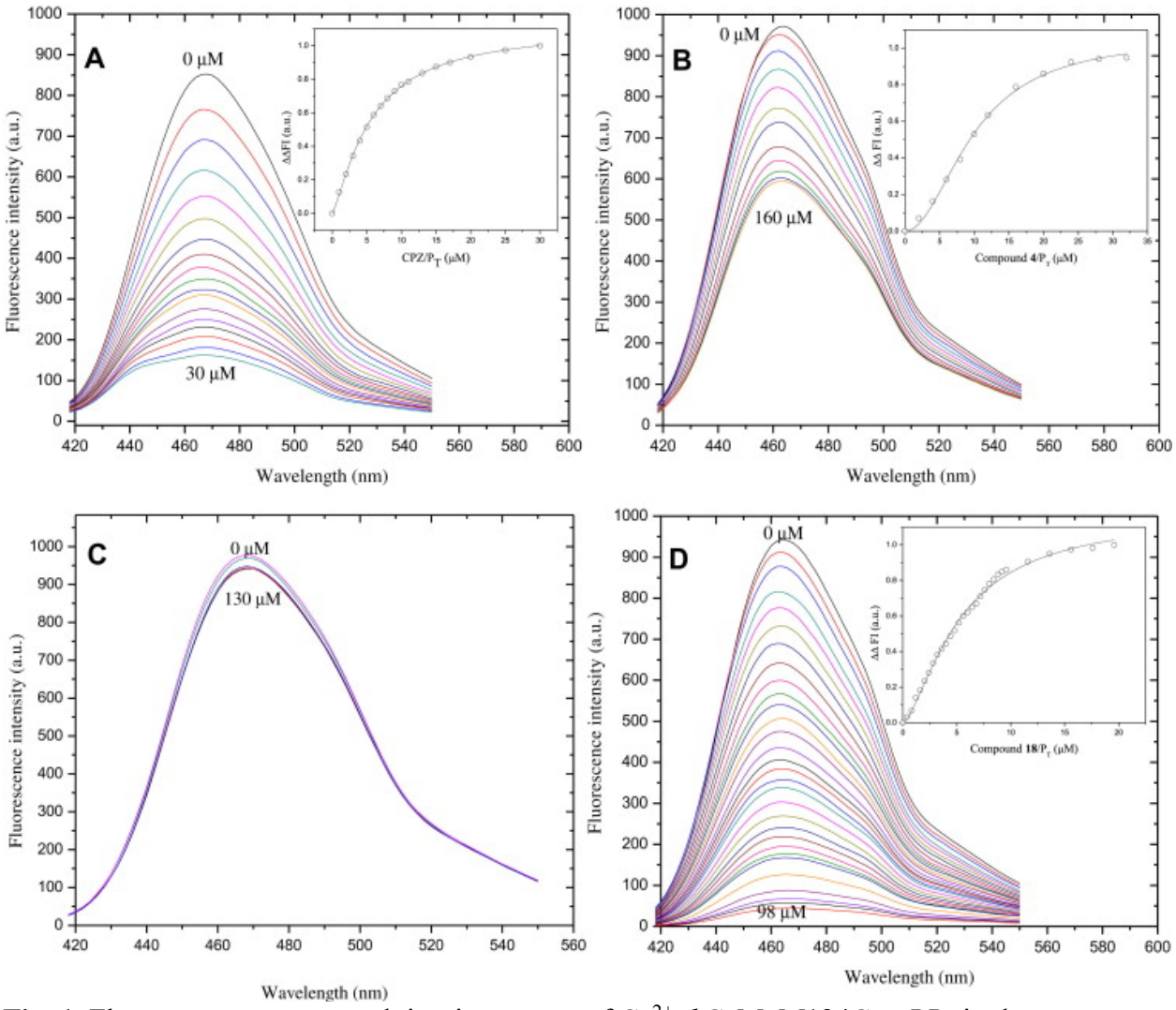

Fig. 1. Fluorescence spectra and titration curves of Ca^{2+}–*h*CaM–M124C–*mBBr* in the presence of CPZ (A), **4** (B), **11** (C), and **18** (D). Buffer was 100 mM of potassium acetate (pH 5.1) at 37 °C and 1 mM $CaCl_2$. Samples were excited at 381 nm, and emission spectra recorded for light scattering effects from 400 to 550 nm. The absolute changes of maximal fluorescence emission ware plotted against the ration compounds/protein total and fitted to the binding equation model to obtain the K_m.

In the enzymatic study, in general the 1,2-diphenylethanes showed a similar trend of effects (Table 1) since compounds **4–6** were among those that clearly inhibited the activation of PDE1 with IC_{50} between 18 and 36 µM. The exception was compound **15** which did not bind to Ca^{2+}–CaM but showed good inhibitory effect of the enzymatic activity of the complex Ca^{2+}–CaM–PDE1. This effect could be due to a direct interaction of **15** with PDE1.

In the group of diphenylmethanes, **13** and **14** showed similar affinity to CaM (K_m values ~33 µM) as well as similar inhibitory effect on enzymatic activity of the complex Ca^{+2}–CaM–PDE1. Compared with all compounds tested, their affinity to CaM was comparable to that of compound **10**.

The 1,3-diphenylpropanes **20**–**22** showed K_m values ranged between 8.7 and 54 μM, being **20** the most affine. Comparison of the K_m values of compounds **21** and **7** indicated that the increment of the chain length between the two phenyl rings increases the affinity to Ca^{+2}–CaM. This difference could be due to the highest conformational flexibility of 1,3-diphenylpropanes in comparison to 1,2-diphenylethanes which allows better coupling of the former group to the protein, as could be inferred from the docking analysis (*vide infra*).

During the preparation of compounds **20** and **22**, chalcones **16**–**19** were obtained as intermediates and thereafter included in this study. The results summarized in Table 1 indicated that intermediates **17** and **18** displayed the highest affinity to Ca^{+2}–CaM among all compounds tested. Indeed, comparison of **1**, **18** and **22**(K_m = 60.8, 5.3 and 54.3 μM) revealed that the presence of a conjugated ketone group between the two phenyl rings significantly increased the affinity for CaM. However, comparison between **16** and **20** (K_m = 10.2 and 8.7 μM) indicated that the substitution pattern in the two rings could be more important that the nature of the chain linking them. The better affinity of compound **17** over the remaining compounds could be also explained in terms of structural energy; thus, according with the docking analysis, **17** shows one hydrogen bond interaction (*vide infra*).

Altogether, the results revealed that among similar compounds those possessing hydrophobic substituents had the best affinity for the complex Ca^{+2}–CaM and better inhibitory effect of the complex Ca^{+2}–CaM–PDE1, being the most relevant compounds 1,2-diphenylethane **4**, chalcones**17** and **18** as well as 1,3-diphenylpropane **20**. In most cases the better affinity for the protein correlated with the inhibitory effect of the enzyme activity.

2.1. Docking

To investigate the binding mode of gigantol (**1**) analogs to CaM (PDB code 1LIN), docking studies were performed using the program AUTODOCK 4.0.2 [15], [16]. Those compounds exhibiting the highest affinity to the protein, according to the fluorescence assay, were selected; accordingly, the structures of compounds **4**, **11**, **13**, **17** and **20** were optimized with the program Gaussian 09 using the density functional theory method (DFT) at the B3LYP/3-21g level. Initially, the ligands were docked to the entire protein; then, the best conformations were docked in a smaller area (grid) in order to refine the results. The compounds analyzed bound to the pocket corresponding to sites **I**, **IV**, **IV** and **IV**, respectively (Fig. 2) as TFP, a classical CaM antagonist [17]. Fig. 2 shows the theoretical binding model of **4**, **13**, **17** and **20**, superimposed with the X-ray structure of the protein with the classical inhibitor TFP. In all cases, regardless of the binding site, one of the two phenyl groups of the scaffold sink in the hydrophobic pockets establishing contact similar to those of TFP or W7, which are classical inhibitors of CaM [18]. In the case of compound **4**, the binding site in the docking model consists of Phe92, Leu105, Met109, Met124, Glu127, Ala128, Val136, and Met144.
Compound **13** binding site comprises Phe19, Leu32, Met51, Glu54, Val55, Ile-53, and Phe68. Compound **17** binding pocket includes Phe19, Leu32, Val35, Met36, Leu39, Gln41, Ile63, Phe68, Met51, Ile52, and Val55. Finally, in the case of **20**, Phe19, Met51, Ile52, Val55, Ile63, Phe68 and Met71 were part of the pocket. Although there are not clear clues of which are the structural features responsible for the affinity of these compounds to CaM, the highest affinity of **17** to the protein might be due to differences in the contact surfaces and/or protein

conformation upon interaction of the ligands, despite some common amino acid residues at the binding sites; additionally this compound show one hydrogen bond interactions between Met51/O and hydroxyl in the position R_2 of **17**. The results of the docking study revealed also those compounds **4**, **13**, **17** and **20** form mainly hydrophobic and/or π–π interactions with the protein as does AAA. In the case of compound **11**, the docking study predicted no binding to the classical CaM binding sites **I**–**IV** (Fig. 2).

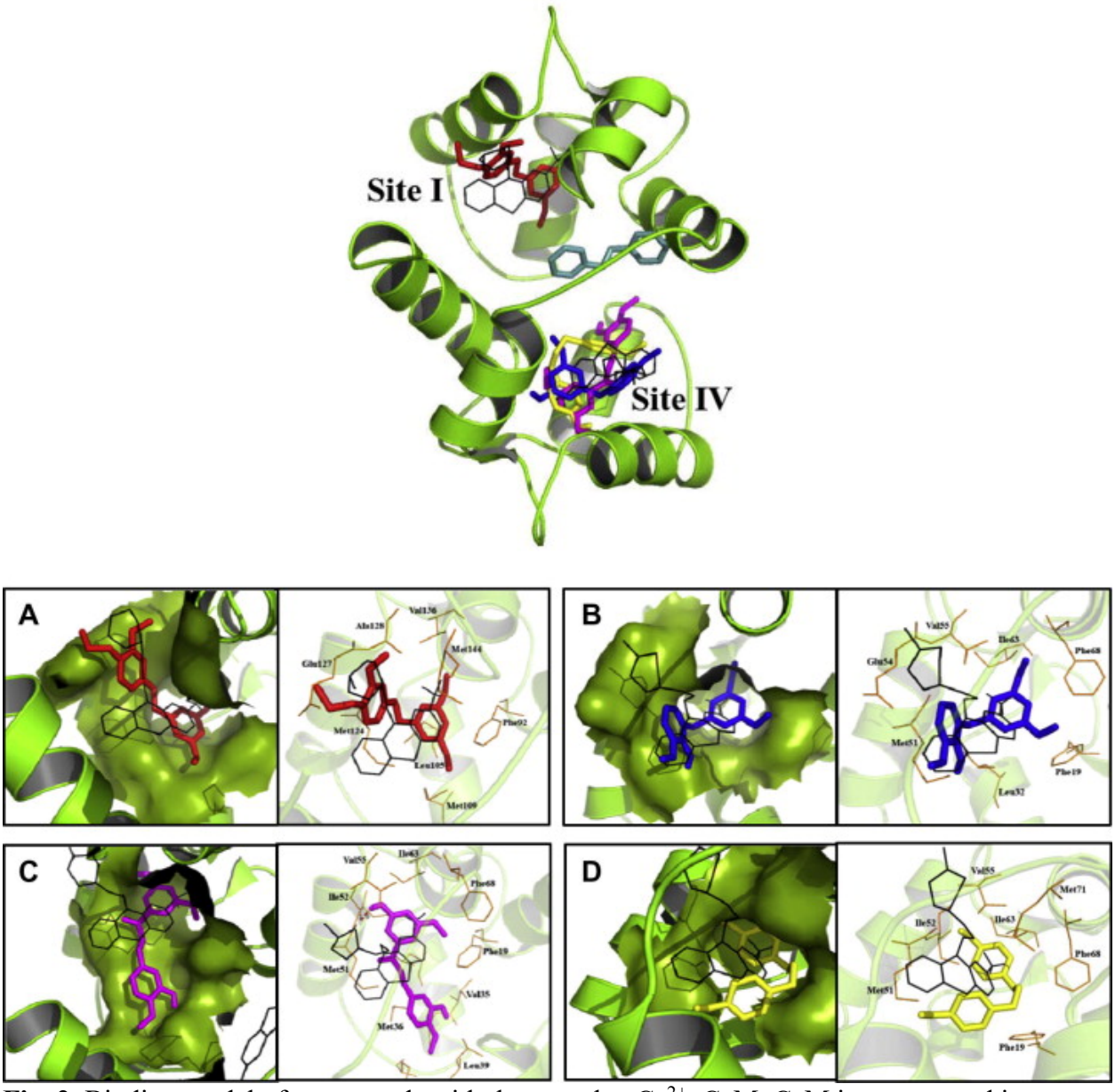

Fig. 2. Binding model of compounds with the complex Ca^{2+}–CaM. CaM is represented in green cartoon. The **TFP** is depicted in black lines, compound **4** in red sticks, **11** in cyan sticks, **13** in blue sticks, **17** in magenta sticks and **20** in yellow stick. Hydrophobic pockets are show in surface and interacting amino acids within the CaM-ligands complex of the compounds **4**(A), **13**(B), **17**(C) and **20**(D). This figure was geared up using the program PyMOL.

3. Conclusions

Several 1,2-diphenylethanes, 1,3-diphenylpropenones, diphenylmethanes, and 1,3-diphenylpropanes with CaM inhibitor properties were discovered. The simplicity and good yields of their synthesis make these compounds good candidates for the development of new CaM-inhibitors. Although there are not clear clues of what are the structural features responsible for the affinity of these compounds to CaM, some of them showed better affinity for the protein than gigantol (**1**) and CPZ [18]. The best ligand was chalcone **17** with a K_m value of 3.89 μM. Among the 1,2-diphenylethanes and 1,3-diphenylpropanes, only derivatives **4**–**6** and **20**, respectively, possessed good affinity to the protein with K_m values approximately six fold than **1**. Compounds **4**, **13**, **17** and **21** bind to CaM in the same region that the classical inhibitors TFP and W-7 mainly through hydrophobic, according to a docking analysis.

Once more the results of our study clearly show that different ligands bind differentially to CaM complexes (Ca^{2+}–CaM or Ca^{2+}–CaM–PDE1) which could have different implications at physiological level. Thus, in the present work compound **15** did not bind to Ca^{2+}–CaM but showed good inhibitory effect of the enzymatic activity of the complex Ca^{2+}–CaM–PDE1; however, further work is needed to demonstrate the **15** selectively bind to the complex Ca^{2+}–CaM–PDE1or to PDE1. The relevance of differentially activate one particular complex could result in selective pharmacological activity and a decrease of side effects of any potential drug.

4. Experimental

4.1. Chemistry

4.1.1. General experimental procedures

Melting points were determined on a Fisher-Johns apparatus and are uncorrected. IR spectra were obtained using KBr disks on a Perkin–Elmer FT 1605 spectrophotometer. NMR spectra were recorded in $CDCl_3$ on a Varian Unity Plus 500 spectrometer either at 300 and 400 (^1H) or 100 (^{13}C) MHz, using tetramethylsilane (TMS) as an internal standard. Electron-impact mass spectra (EIMS) were registered on a JEOL SX 102 mass spectrometer. Open column chromatography was carried out on silica gel 60 (70–230 mesh, Merck, Darmstadt, Germany). Analytical and preparative TLC was performed on precoated silica gel 60 F_{254} plates (Merck, Darmstadt, Germany).

4.1.2. Synthetic intermediates

Diphenylethane (**11**), benzyl phenyl ether (**12**), diphenylmethane (**15**), 4-benzyloxy-3-methoxybenzaldehyde (**24a**), 4-methoxybenzaldehyde (**24b**), 3,4-(methylenedioxy)benzaldehyde (**23c**), 4-ethoxy-3-methoxybenzaldehyde (**24d**), 4-(dimethylamino)benzaldehyde (**24e**), 3-hydroxy-4-methoxybenzaldehyde (**24f**), 4-hydroxy-3-methoxybenzaldehyde (**24g**), 4′-hydroxyacetophenone (**27a**), 3′-hydroxy-5′-methoxyacetophenone (**27b**), 3′-hydroxyacetophenone (**27c**), and guaiacol were purchased from Sigma–Aldrich (St Louis, MO, USA). 3-Benzyloxy-5-methoxybenzyltriphenylphosphonium bromide (**23a**), 3-hydroxybenzyltriphenylphosphonium bromide (**23b**), 3,5-

dimethoxybenzyltriphenylphosphonium bromide (**23c**), and 3,5-dimethoxybenzyl bromide (**25**), were prepared as previously described in Ref. [5].

4.1.3. General procedure for the synthesis of 1,2-diphenylethanes **1**–**10**

The Wittig salt (**23a**–**23c**; 4.4 mmol) and NaH (4.5 mmol) were dissolved in dry tetrahydrofuran (50 mL) under a N_2 atmosphere; then, the appropriated aromatic aldehyde (**24a**–**24e**; 4.4 mmol) was added to the mixture, which was stirred during 3 h at room temperature. After this period of time, water was added and the product extracted with EtOAc. The resulting organic phases were washed with brine and water, dried (anh. Na_2SO_4) and evaporated *in vacuo* to give crude oily residues which were purified by open column chromatography (silica gel; 30 g), hexane-EtOAc to yield a mixture of *Z*- and *E*-stilbenes; the mixture were directly hydrogenated at 60 lb/in^2 (30 °C) in EtOAc (40 mL) over 10% palladium on carbon (0.1 g) for 3 h; the catalyst was then filtered off, and the resulting mixtures evaporated to dryness. These crude reaction mixtures were then purified by open column chromatography to give the final products **1**–**10**. In all cases, for 1 g of crude reaction mixture the chromatographic column was packed with 30 g of silica gel. The eluents consisted in mixtures of hexane-CH_2Cl_2 (1:1 → 0:1) and CH_2Cl_2–MeOH (1:0 → 9:1).

4.1.3.1. 4-[2-(3-Hydroxy-5-methoxyphenyl)ethyl]-2-methoxyphenol **(1)**

The pure compound **1** (0.47 g, yield 41.3%) was obtained as a colorless oil and was identical to a reference standard isolated from *Scaphyglottis livida* (Orchidaceae) [19].

4.1.3.2. 3-Methoxy-5-[2-(4-methoxyphenyl)ethyl]phenol **(2)**

Compound **2** was obtained as an amber oil (0.47 g, yield 41%); UV (MeOH) λ_{max} 276, 208 nm; IR (KBr) ν_{max} 3401, 2933, 1597, 1453, 1244, 1148 cm^{-1}; ^{1}H NMR (400 MHz, $CDCl_3$) δ 2.75–2.85 (4H, m, H-7, H-7′), 3.75 (3H, s, CH_3O-5), 3.79 (3H, s, CH_3O-4′), 4.77 (1H, s, HO-3), 6.25 (2H, d, J = 1.8 Hz, H-2, H-6), 6.32 (1H, t, J = 1.8 Hz, H-4), 6.82 (2H, d, J = 8.8 Hz, H-3′, H-5′), 7.11 (2H, d, J = 8.8 Hz, H-2′, H-6′); ^{13}C NMR (100 MHz, $CDCl_3$) δ 36.8 (C-7′), 38.4 (C-7), 55.5 (CH_3O-4′, CH_3O-5), 99.2 (C-4), 107.0 (C-6), 108.0 (C-2), 113.9 (C-3′, C-5′), 129.5 (C-2′, C-6′), 133.9 (C-1′), 144.8 (C-1), 156.8 (C-4′), 158.1 (C-3), 161.1 (C-5); EM-IE (*m*/*z*) 258 [M$^+$ (65)], 121 (100). HREIMS [M]$^+$(*m*/*z*) 258.1254 (calcd for $C_{16}H_{18}O_3$ 258.1256).

4.1.3.3. 3-[2-(1,3-Benzodioxol-5-yl)ethyl]-5-methoxyphenol **(3)**

Diphenylethane **3** was obtained as yellow crystals (0.74 g, yield 61.7%); mp 115 °C; UV (MeOH) λ_{max} 281, 212 nm; IR (KBr) ν_{max} 3306, 2927, 1592, 1484, 1243 cm^{-1}; ^{1}H NMR (400 MHz, $CDCl_3$) δ 2.75–2.80 (4H, m, H-7, H-7′), 3.75 (3H, s, CH_3O-5), 5.02 (1H, s, HO-3), 5.92 (2H, s, –OCH_2O–), 6.25 (2H, d, J = 2.2 Hz, H-2, H-6), 6.32 (1H, t, J = 2.2 Hz, H-4), 6.63 (1H, dd, J = 7.9, 1.6 Hz, H-6′), 6.65 (1H, d, J = 1.6 Hz, H-5′), 6.72 (1H, d, J = 7.9 Hz, H-2′); ^{13}C NMR (100 MHz, $CDCl_3$) δ 37.2 (C-7′), 38.2 (C-7), 55.2 (CH_3O-3), 99.0 (C-4), 100.7 (–OCH_2O–), 108.1 (C-6), 106.8 (C-2), 107.9 (C-2′), 108.9 (C-5′), 121.2 (C-6′), 135.5 (C-1′), 144.4 (C-1), 145.7 (C-4′), 147.5 (C-3′), 156.5 (C-3), 160.9 (C-5); EM-IE (*m*/*z*) 272 [M$^+$ (44)], 135 (100). HREIMS [M]$^+$(*m*/*z*) 272.1045 (calcd for $C_{16}H_{16}O_4$ 272.1049).

4.1.3.4. 4-[2-(3,5-Dimethoxyphenyl)ethyl]-1-ethoxy-2-methoxybenzene **(4)**

Diphenylethane **4** was obtained as a yellow powder (1.0 g, yield 72.1%); mp 82 °C: UV (MeOH) λ_{max} 279, 208 nm; IR (KBr) ν_{max} 3072, 2935, 1598, 1469, 1136 cm^{-1}; ^1H NMR (400 MHz, $CDCl_3$) δ 1.45 (3H, t, J = 6.8 Hz, $C\underline{H}_3CH_2O$–), 2.84 (4H, br s, H-7, H-7′), 3.76 (6H, s, CH_3O-3, CH_3O-5), 3.83 (3H, s, CH_3O-3′), 4.07 (2H, q, J = 6.8 Hz, $CH_3C\underline{H}_2O$–), 6.31 (1H, t, J = 2.4 Hz, H-4), 6.34 (2H, d, J = 2.4 Hz, H-2, H-6), 6.67 (1H, d, J = 2.0 Hz, H-2′), 6.71 (1H, dd, J = 8.0, 2.0 Hz, H-6′), 6.79 (1H, d, J = 8.0 Hz, H-5′); ^{13}C NMR (100 MHz, $CDCl_3$) δ 14.8 ($\underline{C}H_3CH_2O$–), 37.3 (C-7), 38.4 (C-7′), 55.2 (CH_3O-3, CH_3O-5), 55.8 (CH_3O-3′), 64.3 ($CH_3\underline{C}H_2O$–), 97.8 (C-4), 106.5 (C-2, C-6), 112.0 (C-2′), 112.7 (C-5′), 120.2 (C-6′), 134.3 (C-1′), 144.2 (C-1), 146.4 (C-4′), 149.0 (C-3′), 160.7 (C-3, C-5); EM-IE (*m*/*z*) 316 [M^+ (36)], 165 (100), 137 (70). HREIMS $[M]^+$(*m*/*z*) 316.1670 (calcd for $C_{19}H_{24}O_4$ 316.1675).

4.1.3.5. 3-{2-[4-(Dimethylamino)phenyl]ethyl}-5-methoxyphenol **(5)**

Compound **5** was obtained as a yellow powder (0.57 g, yield 48.2%); mp 146 °C; UV (MeOH) λ_{max} 253, 208 nm; IR (KBr) ν_{max} 3081, 2933, 1599, 1454, 1149 cm^{-1}; ^1H NMR (300 MHz, $CDCl_3$) δ 2.77 (4H, br s, H-7, H-7′), 2.93 (6H, s, $(C\underline{H}_3)_2N$–), 3.75 (3H, s, CH_3O-5), 5.70 (1H, br s, HO-3), 6.20 (1H, br s, H-4), 6.26 (1H, t, J = 2.4 Hz, H-2), 6.32 (1H, br s, H-6), 6.82 (2H, d, J = 8.4 Hz, H-3′, H-5′), 7.09 (2H, d, J = 8.4 Hz, H-2′, H-6′); ^{13}C NMR (75 MHz, $CDCl_3$) δ 36.6 (C-7′), 38.1 (C-7), 41.6 ($(CH_3)_2N$–), 55.2 (CH_3O-5), 98.9 (C-4), 106.6 (C-6), 108.0 (C-2), 114.2 (C-3′, C-5′), 129.1 (C-2′, C-6′), 131.9 (C-1′), 144.6 (C-1), 148.3 (C-4′), 156.8 (C-3), 160.8 (C-5); EM-IE (*m*/*z*) 271 [M^+ (27)], 134 (100), 118 (6). HREIMS $[M]^+$(*m*/*z*) 271.1244 (calcd for $C_{17}H_{21}NO_2$ 271.1572).

4.1.3.6. N-{4-[2-(3,5-Dimethoxyphenyl)ethyl]phenyl}-N,N-dimethylamine **(6)**

Compound **6** was obtained as a white powder (0.77 g, yield 61.8%); mp 41 °C; UV (MeOH) λ_{max} 254, 207 nm; IR (KBr) ν_{max} 3430, 2927, 1596, 1522, 1346, 1159 cm^{-1}; ^1H NMR (400 MHz, $CDCl_3$) δ 2.29 (4H, s, H-7, H-7′), 2.98 (6H, s, $N(CH_3)_2$), 3.76 (6H, s, CH_3O-3, CH_3O-5), 6.28 (1H, m, H-4), 6.64 (2H, m, H-2, H-6), 6.73 (2H, d, J = 8.1 Hz, H-3′, H-5′), 7.12 (2H, d, J = 8.4 Hz, H-2′, H-6′); ^{13}C NMR (100 MHz, $CDCl_3$) δ 37.4 (C-7′), 38.0 (C-7), 41.3 ($N(\underline{C}H_3)_2$), 55.8 (CH_3O-3, CH_3O-5), 97.6 (C-4), 106.5 (C-2, C-6), 112.8 (C-3′, C-5′), 128.6 (C-2′, C-6′), 131.6 (C-1′), 145.1 (C-1), 148.3 (C-4′), 161.5 (C-3, C-5); EM-IE (*m*/*z*) 285 [M^+ (69)], 134 (100), 118 (21). HREIMS $[M]^+$(*m*/*z*) 285.1244 (calcd for $C_{18}H_{23}NO_2$ 285.1729).

4.1.3.7. 3-[2-(1,3-Benzodioxol-5-yl)ethyl]phenol **(7)**

This title compound was prepared following the same general procedure except that two equivalent of NaH (9.0 mmol) was used. Compound **7** was obtained as a yellow powder (0.58 g, yield 54.8%); mp 85 °C; UV (MeOH) λ_{max} 281, 209 nm; IR (KBr) ν_{max} 3367, 2858, 1483, 1244, 1041 cm^{-1}; ^1H NMR (400 MHz, $CDCl_3$) δ 2.82 (4H, s, H-7, H-7′), 4.63 (1H, s, HO-3), 5.92 (2H, s, –OCH_2O–), 6.61 (5H, m, H-2, H-2′, H-3′, H-4, H-6′), 6.75 (1H, m, H-6), 7.14 (1H, m, H-5); ^{13}C NMR (100 MHz, $CDCl_3$) δ 37.4 (C-7′), 38.0 (C-7), 100.7(–OCH_2O–), 108.1 (C-5′), 108.9 (C-2′), 112.8 (C-4), 115.3 (C-2), 120.9 (C-6), 121.2 (C-6′), 129.5 (C-5), 135.5 (C-1′), 143.5 (C-

1), 145.6 (C-4′), 147.5 (C-3′), 155.5 (C-3); EM-IE (*m*/*z*) 242 [M^+ (64)], 135 (100), 105 (8), 77 (22). HREIMS $[M]^+$(*m*/*z*) 242.0941 (calcd for $C_{15}H_{14}O_3$ 242.09243).

4.1.3.8. 1,3-Dimethoxy-5-[2-(4-methoxyphenyl)ethyl]benzene **(8)**

Compound **8** was obtained as an amber oil (0.53 g, yield 44.5%); UV (MeOH) λ_{max} 277, 208 nm; IR (KBr) ν_{max} 2998, 2935, 1596, 1463, 1246, 1153 cm^{-1}; ^1H NMR (300 MHz, $CDCl_3$) δ 2.80–2.87 (4H, m, H-7, H-7′), 3.76 (6H, s, CH_3O-3, CH_3O-5), 3.78 (3H, s, CH_3O-4′), 6.30–6.34 (3H, m, H-2, H-4, H-6), 6.82 (2H, d, *J* = 8.7 Hz, H-3′, H-5′), 7.10 (2H, d, *J* = 8.7 Hz, H-2′, H-6′); ^{13}C NMR (75 MHz, $CDCl_3$) δ 36.7 (C-7), 38.4 (C-7′), 55.21 (CH_3O-3, CH_3O-5), 55.23 (CH_3O-4′), 97.9 (C-4), 106.5 (C-2, C-6), 113.7 (C-3′, C-5′), 129.3 (C-2′, C-6′), 133.8 (C-1), 144.2 (C-1′), 157.8 (C-4′), 160.7 (C-3, C-5); EM-IE (*m*/*z*) 272 [M^+ (24)], 151 (6), 121 (100), 91 (14), 77 (20). HREIMS $[M]^+$(*m*/*z*) 272.1410 (calcd for $C_{17}H_{20}O_3$ 272.1412).

4.1.3.9. 3-[2-(4-Ethoxy-3-methoxyphenyl)ethyl]phenol **(9)**

This title compound was prepared following the same general procedure except that two equivalent of NaH (9.0 mmol) was used. Compound **9** was obtained as yellow crystals (0.67 g, yield 56.3%); mp 54 °C; UV (MeOH) λ_{max} 279, 207 nm; IR (KBr) ν_{max} 3536, 2944, 1590, 1516, 1362, 1229 cm^{-1}; ^1H NMR (400 MHz, $CDCl_3$) δ 1.45 (3H, t, *J* = 7.0 Hz, $C\underline{H}_3CH_2O$–), 2.84 (4H, s, H-7, H-7′), 3.84 (3H, s, CH_3O-3), 4.07 (2H, q, *J* = 7.0 Hz, $CH_3C\underline{H}_2O$–), 4.82 (1H, br s, HO-3), 6.64–6.66 (2H, m, H-2′, H-4), 6.66–6.72 (2H, m, H-2, H-6), 6.75 (1H, d, *J* = 7.5 Hz, H-6′), 6.79 (1H, d, *J* = 7.5 Hz, H-5′), 7.14 (1H, td, *J* = 7.5, 1.2 Hz, H-5); ^{13}C NMR (100 MHz, $CDCl_3$) δ 14.8 ($\underline{C}H_3CH_2O$–), 37.3 (C-7), 37.9 (C-7′), 55.8 (CH_3O–), 64.3 ($CH_3\underline{C}H_2O$–), 112.0 (C-2′), 112.8 (C-4), 115.4 (C-2, C-5′), 120.2 (C-6), 120.9 (C-6′), 129.4 (C-5), 134.3 (C-1′), 143.7 (C-1), 146.4 (C-4′), 148.9 (C-3′), 155.5 (C-3); EM-IE (*m*/*z*) 272 [M^+ (37)], 165 (96), 137 (100), 107 (15), 77 (10). HREIMS $[M]^+$(*m*/*z*) 272.1414 (calcd for $C_{17}H_{20}O_3$ 272.1412).

4.1.3.10. 3-[2-(4-Ethoxy-3-methoxyphenyl)ethyl]-5-methoxyphenol **(10)**

Compound **10** was obtained as an amber oil (0.81 g, yield 60.8%): UV (MeOH) λ_{max} 280, 208 nm; IR (KBr) ν_{max} 3451, 2935, 1600, 1456, 1145 cm^{-1}; ^1H NMR (400 MHz, $CDCl_3$) δ 1.45 (3H, t, *J* = 7.1 Hz, $C\underline{H}_3CH_2O$–), 2.82 (4H, br s, H-7, H-7′), 3.75 (3H, s, CH_3O-3′), 3.85 (3H, s, CH_3O-3), 4.07 (2H, q, *J* = 7.1 Hz, $CH_3C\underline{H}_2O$–), 4.82 (1H, s, HO-3), 6.25 (2H, d, *J* = 1.8 Hz, H-2, H-6), 6.32 (1H, t, *J* = 1.8 Hz, H-4), 6.66 (1H, d, *J* = 2.0 Hz, H-2′), 6.69 (1H, dd, *J* = 8.1, 2.0 Hz, H-6′), 6.79 (1H, d, *J* = 8.1 Hz, H-5′); ^{13}C NMR (100 MHz, $CDCl_3$) δ 15.1 ($\underline{C}H_3CH_2O$–), 37.4 (C-7′), 38.4 (C-7), 55.5 (CH_3O-3), 56.2 (CH_3O-3′), 64.7 ($CH_3\underline{C}H_2O$–), 99.3 (C-4), 107.1 (C-6), 108.2 (C-2), 112.6 (C-2′), 113.3 (C-5′), 120.6 (C-6′), 134.6 (C-1′), 144.8 (C-1), 146.8 (C-4′), 149.4 (C-3′), 156.8 (C-3), 161.2 (C-5); EM-IE (*m*/*z*) 302 [M^+ (38)], 165 (90), 137 (100), 122 (19), 94 (32), 77 (30). HREIMS $[M]^+$(*m*/*z*) 302.1512 (calcd for $C_{18}H_{22}O_4$ 302.1518).

4.1.4. Synthesis of diphenylmethanes **13** and **14**

4.1.4.1. Synthesis of intermediate 1,3-dimethoxy-5-[(2-methoxyphenoxy)methyl]benzene **(26)**

To a solution of 8.5 g (36.8 mmol) of 3,5-dimethoxybenzyl bromide (**25**) in acetone (65 mL), 5.0 g (40.3 mmol) of guaiacol, 5.5 g (39.9 mmol) of K_2CO_3, and 1.0 g (6.1 mmol) of KI were added. The mixture was stirred and heated to reflux for 10 h; afterward, the solvent was removed *in vacuo*. To the previous resulting mixture 30 mL of water were added at room temperature and extracted with EtOAc (2 × 25 mL). The combined organic layers were consecutively washed with an aqueous solution of NaOH (5%, 20 mL), and brine (2 × 25 mL), and finally dried over anh. Na_2SO_4. After elimination of the solvent *in vacuo*, the crude reaction mixture was purified by flash column chromatography on silica gel (hexane-EtOAc, 9:1; for 1.0 g of crude reaction, 30 g of silica gel were packed in the column) to give compound **26** (6.72 g, yield 66.7%). UV (MeOH) λ_{max} 275, 207 nm; IR (KBr) ν_{max} 2939, 2837, 1598, 1505, 1456, 1251 cm^{-1}; ^1H NMR (400 MHz, $CDCl_3$) δ 3.78 (6H, s, CH_3O-3, CH_3O-5), 3.89 (3H, s, CH_3O-2′), 5.10 (2H, s, –CH_2O–), 6.38 (1H, t, J = 2.4 Hz, H-4), 6.60 (2H, d, J = 2.4 Hz, H-2, H-6), 6.81–6.95 (4H, m, ArH); ^{13}C NMR (100 MHz, $CDCl_3$) δ 55.3 (CH_3O-3, CH_3O-5), 55.9 (CH_3O-2′), 71.0 (–CH_2O–), 99.8 (C-4), 104.9 (C-2, C-6), 111.9 (C-3′), 114.3 (C-6′), 120.8 (C-4′), 121.5 (C-5′), 139.8 (C-1), 148.1 (C-2′), 149.7 (C-1′), 160.9 (C-3, C-5); EM-IE (*m*/*z*) 274 [M^+ (27)], 151 (100), 77 (43).HREIMS $[M]^+$(*m*/*z*) 274.1204 (calcd for $C_{16}H_{18}O_4$ 274.1205).

4.1.4.2. 2-(3,5-Dimethoxybenzyl)-6-methoxyphenol (13) and 4-(3,5-dimethoxybenzyl)-2-methoxyphenol **(14)**

1.5 g (5.5 mmol) of **26**, 1.7 mL (29.1 mmol) of H_3PO_4, and 18 mL of toluene were mixed at room temperature. The mixture was stirred and heated under reflux for 6.5 h. The resulting solution was allowed to cool to room temperature; then, 15 mL of water and Na_2CO_3, to pH 12, were added to the reaction mixture, from which the crude products were extracted with EtOAc (2 × 15 mL). The combined organic layers were washed with brine (10 mL), and dried (Na_2SO_4). After solvent removal, the residue was purified by flash chromatography (hexane-EtOAc, 9:1; for 1.0 g of crude reaction, 30 g of silica gel were packed in the column) to give products diphenylmethane **13** (0.4 g, yield 26.8%) as yellow powder mp 80 °C, and **14** as a colorless oil (36 mg, yield 2.4%). **13**: UV (MeOH) λ_{max} 273, 226 nm; IR (KBr) ν_{max} 3406, 2957, 1590, 1468, 1208, 1159 cm^{-1}; ^1H NMR (400 MHz, $CDCl_3$) δ 3.74 (3H, s, CH_3O-3′), 3.75 (6H, s, CH_3O-3, CH_3O-5), 3.95 (2H, s, –CH_2–), 5.52 (1H, br s, HO-2′), 6.31 (1H, t, J = 2.3 Hz, H-4), 6.35 (2H, d, J = 2.3 Hz, H-2, H-6), 6.66 (1H, dd, J = 8.0, 1.7 Hz, H-6′), 6.84 (1H, dd, J = 8.0, 1.7 Hz, H-4′), 6.94 (1H, t, J = 8.0 Hz, H-5′); ^{13}C NMR (100 MHz, $CDCl_3$) δ 35.7 (–CH_2–), 55.2 (CH_3O-3, CH_3O-5), 61.3 (CH_3O-3′), 97.9 (C-4), 107.0 (C-2, C-6), 113.9 (C-4′), 122.4 (C-5′), 124.9 (C-6′), 133.5 (C-1′), 142.9 (C-1), 145.4 (C-2′), 148.9 (C-3′), 160.8 (C-3, C-5); EM-IE (*m*/*z*) 274 [M^+ (100)], 151 (72.5), 115 (41). HREIMS $[M]^+$(*m*/*z*) 274.1206 (calcd for $C_{16}H_{18}O_4$ 274.1205). **14**: UV (MeOH) λ_{max} 280, 219 nm; IR (KBr), ν_{max} 3437, 2935, 1594, 1511, 1460, 1152 cm^{-1}; ^1H NMR (400 MHz, $CDCl_3$): δ 3.75 (6H, s, CH_3O-3, CH_3O-5), 3.88 (3H, s, CH_3O-3′), 3.94 (2H, s, –CH_2–), 5.72 (1H, s, HO-4′), 6.30 (1H, t, J = 2.4 Hz, H-4), 6.43 (2H, d, J = 2.4 Hz, H-2, H-6), 6.72, (1H, dd, J = 6.8, 2.4 Hz, H-6′), 6.74–6.80 (2H, m, H-2′, H-5′); ^{13}C NMR (100 MHz, $CDCl_3$): δ 35.6 (–CH_2–), 55.2 (CH_3O-3, CH_3O-5), 56.0 (CH_3O-3′), 97.8 (C-4), 107.0 (C-2, C-6), 108.7 (C-2′), 119.4 (C-5′), 122.7 (C-6′) 126.6 (C-1′), 143.2 (C-1), 143.4 (C-4′), 146.4 (C-3′), 160.6 (C-3, C-5); EM-IE (*m*/*z*) 274 [M^+ (29)], 151 (100), 115 (20.5). HREIMS $[M]^+$(*m*/*z*) 274.1200 (calcd for $C_{16}H_{18}O_4$ 274.1205).

4.1.5. General procedure for the synthesis of 1,3-diphenylpropenones **16**–**19**

Equimolar portions of acetophenones **27a–27c** (10 mmol) and aromatic aldehydes **24b**, **24c** or **24g** (10 mmol) were dissolved in ethanol (15 mL). 5 mL of a 40% aqueous KOH solution was then slowly added drop wise. The mixture was stirred and heated to reflux for 10 h. The mixture of reaction was poured into ice-water and acidified with cold diluted HCl (2N). The precipitate was filtered and purified by flash column chromatography on silica gel (hexane-EtOAc, 9:1) to give the final products **16–19**. For 1.0 g of crude reaction, 30 g of silica gel were packed in the column.

4.1.5.1. (2*E*)-1-(4-hydroxyphenyl)-3-(4-methoxyphenyl)prop-2-en-1-one **(16)**

Compound **16** (1.96 g, yield 77.4%) was obtained as yellow powder; mp 190 °C; UV (MeOH) λ_{max} 344, 236 nm; IR (KBr) ν_{max} 3123, 2839, 1645, 1563, 1429, 1166 cm^{-1}; ^1H NMR (400 MHz, $CDCl_3$) δ 3.89 (3H, s, CH_3O-4), 4.89 (1H, s, HO-4′), 6.96–6.98 (4H, m, H-3, H-3′, H-5, H-5′), 7.45 (1H, d, J = 15.6 Hz, =CH-α), 7.63 (2H, d, J = 8.7 Hz, H-2, H-6), 7.81 (1H, d, J = 15.9 Hz, =CH-β), 8.03 (2H, d, J = 8.7 Hz, H-2′, H-6′); ^{13}C NMR (100 MHz, $CDCl_3$) δ 55.4 (CH_3O-4), 114.4 (C-3, C-5), 115.4 (C-3′, C-5′), 119.5 (C-α), 127.7 (C-1), 130.1 (C-1′), 130.7 (C-2, C-6), 131.0 (C-2′, C-6′), 144.1 (C-β), 159.7 (C-4), 161.6 (C-4′), 188.9 (C=O); EM-IE (*m*/*z*) 254 [M^+ (100)], 239 (21), 161 (18), 121 (20). HREIMS $[M]^+$(*m*/*z*) 254.0950 (calcd for $C_{16}H_{14}O_3$ 254.0943).

4.1.5.2. (2*E*)-3-(3-hydroxy-4-methoxyphenyl)-1-(3-hydroxy-5-methoxyphenyl)prop-2-en-1-one **(17)**

Chalcone**17** (2.16 g, yield 72.0%) was obtained as yellow powder; mp 161 °C; UV (MeOH) λ_{max} 356, 207 nm; IR (KBr) ν_{max} 3476, 3263, 2840, 1646, 1562, 1266 cm^{-1}; ^1H NMR (400 MHz, CD_3OD) δ 3.82 (3H, s, CH_3O-4), 3.91 (3H, s, CH_3O-5′), 6.60 (1H, t, J = 2.1 Hz, H-4′), 6.98 (1H, d, J = 8.3 Hz, H-5), 7.01–7.03 (2H, m, H-2′, H-6′), 7.19 (1H, dd, J = 8.3, 2.1 Hz, H-6), 7.21 (1H, d, J = 2.1 Hz, H-2), 7.41 (1H, d, J = 15.7 Hz, =CH-α), 7.67 (1H, d, J = 15.7 Hz, =CH-β); ^{13}C NMR (100 MHz, CD_3OD) δ 54.5 (CH_3O-5′), 54.9 (CH_3O-4), 104.6 (C-6′), 105.5 (C-4′), 107.6 (C-2′), 111.1 (C-5), 113.7 (C-2), 119.4 (C-α), 122.14 (C-6), 127.9 (C-1), 140.7 (C-1′), 145.4 (C-β), 146.6 (C-3), 150.5 (C-4), 158.7 (C-3′), 161.2 (C-5′), 191.0 (C=O); EM-IE (*m*/*z*) 300 [M^+ (100)], 285 (34), 177 (35), 142 (41). HREIMS $[M]^+$(*m*/*z*) 300.0980 (calcd for $C_{17}H_{16}O_5$ 300.0998).

4.1.5.3. (2*E*)-1-(3-hydroxy-5-methoxyphenyl)-3-(4-hydroxy-3-methoxyphenyl)prop-2-en-1-one **(18)**

Chalcone **18** (1.91 g, yield 63.7%) was obtained as yellow powder; mp 161–162 °C; UV (MeOH) λ_{max} 360, 207 nm; IR (KBr) ν_{max} 3407, 2943, 1648, 1565, 1428, 1149 cm^{-1}; ^1H NMR (400 MHz, CD_3OD) δ 3.83 (3H, s, CH_3O-3), 3.93 (3H, s, CH_3O-5′), 6.60 (1H, t, J = 2.0 Hz, H-4′), 6.84 (1H, d, J = 8.4 Hz, H-6), 7.04 (1H, t, J = 2.0 Hz, H-2′), 7.06 (1H, t, J = 2.0 Hz, H-6′), 7.22 (1H, dd, J = 8.4, 2.0 Hz, H-5), 7.33 (1H, d, J = 2.0 Hz, H-2), 7.46 (1H, d, J = 15.6 Hz, =CH-α), 7.71 (1H, d, J = 15.6 Hz, =CH-β); ^{13}C NMR (100 MHz, CD_3OD) δ 54.5 (CH_3O-5′), 55.1 (CH_3O-3), 104.7 (C-2′), 105.4 (C-4′), 107.6 (C-6′), 110.8 (C-2), 115.2 (C-5), 118.8 (C-α), 123.5 (C-6), 126.8 (C-1), 140.3 (C-1′), 145.9 (C-β), 148.0 (C-4), 149.7 (C-3), 158.6 (C-3′), 161.1

(C-5′), 191.2 (C═O); EM-IE (*m*/*z*) 300 [M^+ (100)], 177 (28), 145 (23). HREIMS $[M]^+$(*m*/*z*) 300.0980 (calcd for $C_{17}H_{16}O_5$ 300.0998).

4.1.5.4. (2*E*)-3-(1,3-benzodioxol-5-yl)-1-(3-hydroxyphenyl)prop-2-en-1-one **(19)**

To a solution of (1.36 g, 10 mmol) 4′-hydroxyacetophenone (**27c**), (1.5 g, 10 mmol) of 3,4-(methylenedioxy)benzaldehyde (**24c**) in ethanol (15 mL), an aqueous solution of KOH (40%, 5 mL) was added slowly. The mixture was stirred and heated to reflux for 10 h, and then the suspension was poured into ice-water. The precipitate was filtered and dried to yield (*E*)-3′-hydroxy-3,4-methylenedioxydiphenylpropenone (**19**) (1.7 g, 63.7%) as an amorphous yellow powder; UV (MeOH) λ_{max} 361, 206 nm; IR (KBr) ν_{max} 3406, 2945, 1644, 1563 cm^{-1}; ^1H NMR (400 MHz, $CDCl_3$) δ 5.18 (1H, br s, HO-3′), 6.07 (2H, s, –OCH_2O–), 6.89 (1H, d, *J* = 7.9 Hz, H-5), 6.92 (1H, dd, *J* = 7.3, 3.8 Hz, H-4′), 7.09 (1H, dd, *J* = 8.2, 1.6 Hz, H-6′), 7.18 (1H, dd, *J* = 7.9, 1.8 Hz, H-6), 7.27 (1H, d, *J* = 2.0 Hz, H-2), 7.37 (1H, dd, *J* = 5.6, 4.9 Hz, H-2′), 7.45 (1H, d, *J* = 15.6 Hz, ═CH-α),7.59 (1H, t, *J* = 7.8 Hz, H-5′),7.88 (1H, d, *J* = 15.8 Hz, ═CH-β). HREIMS $[M]^+$(*m*/*z*) 268.2639 (calcd for $C_{16}H_{12}O_4$ 268.2640).

4.1.6. Synthesis of 1,3-diphenylpropanes **20**–**22**

4.1.6.1. 4-[3-(4-Methoxyphenyl)propyl]phenol **(20)**

Chalcone **16** (3.0 g) was dissolved in a solution of H_2SO_4 (2.0 mL) in EtOH (100 mL) and hydrogenated at 60 lb/in^2 (60 °C) over 10% palladium on carbon (0.3 g) for 4 h; the catalyst was filtered and the solvent removed *in vacuo*. The resulting solution was then tried with 50 mL of water and the crude products were extracted with EtOAc (2 × 25 mL). The combined organic layers were washed with brine (20 mL), and dried (Na_2SO_4). After solvent removal, the residue was purified by flash chromatography to give diphenylpropane **20**: (2.67 g, yield 92.4%) as yellow powder; mp 48 °C; UV (MeOH) λ_{max} 277, 226 nm; IR (KBr) ν_{max} 3418, 2941, 1608, 1512, 1353, 1216 cm^{-1}; ^1H NMR (400 MHz, $CDCl_3$) δ 1.80–1.90 (2H, m, H-8), 2.50–2.60 (4H, m, H-7, H-7′), 3.78 (3H, s, CH_3O-4′), 4.41 (1H, br s, HO-4), 6.73 (2H, d, *J* = 8.8 Hz, H-3, H-5), 6.82 (2H, d, *J* = 8.8 Hz, H-3′, H-5′), 7.02 (2H, d, *J* = 8.8 Hz, H-2, H-6), 7.08 (2H, d, *J* = 8.8 Hz, H-2′, H-6′); ^{13}C NMR (100 MHz, $CDCl_3$) δ 33.4 (C-8), 34.8 (C-7, C-7′), 55.3 (CH_3O-4′), 113.7 (C-3′, C-5′), 115.1 (C-3, C-5), 129.3 (C-2′, C-6′), 129.4 (C-2, C-6), 134.4 (C-1′), 134.5 (C-1), 153.5 (C-4), 157.5 (C-4′); EM-IE (*m*/*z*) 242 [M^+ (71)], 135 (18), 121 (100), 107 (24). HREIMS $[M]^+$(*m*/*z*) 242.1301 (calcd for $C_{16}H_{18}O_2$ 242.1307).

4.1.6.2. 4-[3-(1,3-Benzodioxol-5-yl)propyl]phenol **(21)**

Compound **19** (1.5 g, 5.6 mmol) was dissolved in a solution of H_2SO_4 (1.0 mL) in EtOH (50 mL), and hydrogenated at 60 lb/in^2 (60 °C) over 10% palladium on carbon (0.15 g) for 4 h. The catalyst was filtered off and the filtrate evaporated. The resulting solution was then tried with 25 mL of water and the crude products were extracted with EtOAc (2 × 25 mL). The combined organic layers were washed with brine (20 mL), and dried (Na_2SO_4). After solvent removal, the residue was purified by flash chromatography to give diphenylpropane **21** (1.48 g, yield 58%) as yellow powder; mp 84 °C: UV (MeOH) λ_{max} 281, 209 nm; IR (KBr) ν_{max} 3477, 3368, 2928, 1586, 1500, 1483, 1244 cm^{-1}; ^1H NMR (400 MHz, $CDCl_3$) δ 1.26 (2H, m, H-8),

2.82 (4H, s, H-7, H-7′), 4.63 (1H, br s, HO-3), 5.92 (2H, s, –OCH_2O–), 6.61 (1H, dd, J = 8.0, 1.6 Hz, H-6′), 6.64–6.68 (3H, m, H-2, H-2′, H-4), 6.72 (1H, d, J = 8.0 Hz, H-5′), 6.75 (1H, d, J = 7.6 Hz, H-6), 7.14 (1H, dt, J = 7.6, 2.4 Hz, H-5); ^{13}C NMR (100 MHz, $CDCl_3$) δ 37.4 (C-8), 37.9 (C-7, C-7′), 100.7 (–OCH_2O–), 108.1 (C-5′), 112.5 (C-2′), 112.8 (C-4), 115.3 (C-2), 120.9 (C-6), 121.1 (C-6′), 129.5 (C-5), 135.5 (C-1′), 143.6 (C-1), 145.6 (C-4′), 147.5 (C-3′), 155.4 (C-3); EM-IE (*m*/*z*) 256 [M^+ (60)], 149 (100), 119 (16). HREIMS $[M]^+$(*m*/*z*) 256.1090 (calcd for $C_{16}H_{16}O_3$ 256.1099).

4.1.6.3. 4-[3-(3-Hydroxy-5-methoxyphenyl)propyl]-2-methoxyphenol **(22)**

Compound **22** (crystalline solid, mp 77 °C, 0.25 g, yield 54.2%) was prepared from chalcone **18** (0.48 g) following the method described for **21**. UV (MeOH) λ_{max} 279, 207 nm; IR (KBr) ν_{max} 3355, 3039, 2931, 1611, 1591, 1513, 1455, 1196, 813 cm^{-1}; ^{1}H NMR (400 MHz, $CDCl_3$) δ 1.89 (2H, q, J = 7.6 Hz, H-8), 2.55 (2H, t, J = 7.6 Hz, H-7), 2.56 (2H, t, J = 7.6 Hz, H-7′), 3.76 (3H, s, CH_3O-3′), 3.86 (3H, s, CH_3O-5), 5.49 (2H, br s, HO-3, HO-4′), 6.24 (2H, m, H-2, H-4), 6.32 (1H, d, J = 3.0 Hz, H-2′), 6.67 (2H, m, H-6, H-6′), 6.83 (1H, d, J = 8.0 Hz, H-5′). ^{13}C NMR (100 MHz, $CDCl_3$) δ 32.8 (C-8), 35.0 (C-7, C-7′), 35.4 (C-7, C-7′), 55.2 (CH_3O-3′), 55.9 (CH_3O-5), 98.2 (C-4), 106.8 (C-6), 107.9 (C-2), 111.0 (C-2′), 114.2 (C-5′), 120.9 (C-6′), 134.2 (C-1′), 143.6 (C-1), 145.1 (C-4′), 146.3 (C-3′), 156.6 (C-3), 160.8 (C-5); EM-IE (*m*/*z*) 288 [M^+ (9)], 150 (4), 138 (100), 122 (4), 77 (7), 65 (4). HREIMS $[M]^+$(*m*/*z*) 288.3378 (calcd for $C_{17}H_{20}O_4$ 288.3380).

4.2. Biological study

4.2.1. Phosphodiesterase activity assay

Phosphodiesterase activity was measured according to the method described by Rivero and coworkers with some modifications [12]. Briefly, CaM (0.08 μg) was incubated with 0.015 units of PDE1 from bovine brain during 30 min in 40 μL of assay solution containing 0.063 units of 5′-nucleotidase (*Crotalus atrox* venom from Sigma), 45 mM Tris–HCl, 5.6 mM magnesium acetate, 45 mM imidazole, 2.5 mM calcium chloride and 10 mM BSA, pH 7.0. Tested compounds were then added to the assay medium at 0.5, 1, 2, 3, 4, 7, 13, 20, 32, 50, and 65 mM in MeCN-water (1:1), and the samples incubated during 30 min; thereafter 10 μL of 10.8 mM *c*AMP were added to start the assay. After 15 min, the assay was stopped by the addition of 190 μL of malachite green solution. The amount of inorganic phosphate released was measured at 700 nm, correlated with the activity of the PDE1. All the results are expressed as the mean of at least six experiments ± SEM. The IC_{50} (concentration inhibiting by 50% the activity of the enzyme) values were determined by non-linear regression analysis by fitting to hyperbolic inhibition.

4.2.2. Steady-state fluorescence (biosensor CaM)

All measurements were conducted with an ISS-PC1 spectrofluorometer (ISS, Champaign, IL), with sample stirring at 37 °C. The protein *h*CaM M124C–*mBBr* (5 μM) [14] was incubated in a phosphate buffer (100 mM; pH 5.1) and 10 mM $CaCl_2$. Fluorescence emission spectra were acquired with excitation and emission slit widths of 4 and 8 nm, respectively. The excitation

wavelength was 381 nm and emission wavelengths were measured from 400 to 550 nm. The fractional degree of saturated *h*CaM M124C–*mBBr* with ligand (y), was calculated by changes in fluorescence upon ligand binding according to $y = (F - F_0)/(F_\infty - F_0)$, where F_∞ represents the fluorescence intensity at saturation of the ligand, y was plotted as a function of the inhibitor concentration, and the apparent constants (K_m) concentration that produces an effect that is 50% of maximum effect (E_{max}) were obtained by fitting to equation [20].

$$y = \frac{E_{max} L^h}{K_m^h + L^h}$$

where y represents the fractional degree of fluorescence intensity at 470 nm, K_m is the apparent constant for the ligands, E_{max} is the maximal value of effect, L is the concentrations of the ligand and h is the Hill coefficient. The data were analyzed using the program Origin 8.0 (OriginLab, Northampton, MA).

4.3. Docking

To generate more accurate and physically realistic models of the protein CaM (PDB code 1LIN), after several iterations of rebuilding and refinement, we perform a final all-atom refinement of CaM with the idealization application of the Rosetta3.1 release [21]. This application rebuilds molecules using ideal bond lengths, bond angles, and torsion angles. The starting conformation of the ligands was optimized using the program Gaussian 09, revision A.02 (Gaussian Inc., Wallingford, CT) at DTF B3LYP/3-21g level of theory. Blind docking was carried out using AutoDock4 version 4.2 software (http://autodock.scripps.edu/) [15], [16] using the default parameters the Lamarkian genetic algorithm with local search, number of individuals in population (150), maximum number of energy evaluations (2.5 million), maximum number of generations (27 000), rate of gene mutation (0.02), rate of crossover (0.8) and 100 runs for docking. The initial grid box size was 60 Å × 60 Å × 60 Å in the x, y and z dimensions. The refined docking analysis was performed in a smaller grid box, with 30 Å × 30 Å × 30 Å dimensions, centered in the ligand. All calculations were made using a parallel distributed memory supercomputer (Kanbalam, Dirección General de Cómputo y de Tecnologías de Información y Comunicación, UNAM) which contains 1368 processors AMD Opteron, around 3 terabyte of memory and 160 terabyte of storage (http://www.super.unam.mx/).

Acknowledgments

This work was supported by grants from DGAPA-UNAM (IN223509) and CONACyT 99395. We thank Georgina Duarte, Margarita Guzmán, Nuria Esturau, Marisela Gutierrez, Isabel Rivero, and Araceli Pérez for their valuable technical assistance. The authors are very grateful to Dr. A. Olson and his colleagues at the Scripps Research Institute for providing AutoDock. Martha Leyte-Lugo acknowledges a fellowship from CONACyT. Martin González-Andrade and Adelfo Reyes acknowledge postdoctoral and sabbatical fellowships, respectively, awarded by DGAPA-UNAM. We are indebted to Dirección General de Cómputo y de Tecnologías de Información y Comunicación, UNAM, for providing the resources to carry out computational calculations through KanBalam System.

Appendix. Supplementary data

Supplementary data (NMR spectra) associated with this articlecan be found, in the online version atdoi:10.1016/j.ejmech.2011.03.057

References

[1] S. Estrada, A. Rojas, Y. Mathison, A. Israel, R. Mata, Nitric oxide/cGMP mediates the spasmolytic action of 3,40-dihydroxy-5,50-dimethoxybibenzyl from scaphyglottis livida, Planta Med. 65 (1999) 109e114.

[2] M. Deciga-Campos, J.F. Palacios-Espinosa, A. Reyes-Ramirez, R. Mata, Antinociceptive and anti-inflammatory effects of compounds isolated from Scaphyglottis livida and Maxillaria densa, J. Ethnopharmacol 114 (2007) 161e168.

[3] S. Estrada-Soto, J.J. Lopez-Guerrero, R. Villalobos-Molina, R. Mata, Endothelium-independent relaxation of aorta rings by two stilbenoids from the orchids Scaphyglottis livida, Fitoterapia 77 (2006) 236e239.

[4] Y. Hernandez-Romero, L. Acevedo, M.D. Sanchez, W.T. Shier, H.K. Abbas, R. Mata, Phytotoxic activity of bibenzyl derivatives from the orchid Epidendrum rigidum, J. Agr Food Chem. 53 (2005) 6276e6280.

[5] Y. Hernandez-Romero, J.I. Rojas, R. Castillo, A. Rojas, R. Mata, Spasmolytic effects, mode of action, and structure-activity relationships of stilbenoids from Nidema boothii, J. Nat. Prod. 67 (2004) 160e167.

[6] W.Y. Cheung, Calmodulin plays a pivotal role in cellular-regulation, Science 207 (1980) 19e27.

[7] I. Kovesi, D.K. Menyhard, M. Laberge, J. Fidy, Interaction of antagonists with calmodulin: insights from molecular dynamics simulations, J. Med. Chem. 51 (2008) 3081e3093.

[8] P.L. Majumder, S. Pal, S. Majumder, Dimeric phenanthrenes from the orchid Bulbophyllum reptans, Phytochemistry 50 (1999) 891e897.

[9] F. Orsini, L. Verotta, M. Lecchi, R. Restano, G. Curia, E. Redaelli, E. Wanke, Resveratrol derivatives and their role as potassium channels modulators, J. Nat. Prod. 67 (2004) 421e426.

[10] L.S. Hart, C.R. Waddington, Aromatic Rearrangements in the benzene series 4. Intramolecularity of both the ortho-rearrangement and para-rearrangement of benzyl phenyl ether as shown by labeling experiments, J Chem Soc Perk T 2 (1985) 1607e1612.

[11] X. Yang, W. Wang, J. Tan, D. Song, M. Li, D. Liu, Y. Jing, L. Zhao, Synthesis of a series of novel dihydroartemisinin derivatives containing a substituted chalcone with greater cytotoxic effects in leukemia cells, Bioorg. Med. Chem. Lett. 19 (2009) 4385e4388.

[12] B. Rivero-Cruz, I. Rivero-Cruz, R. Rodriguez-Sotres, R. Mata, Effect of natural and synthetic benzyl benzoates on calmodulin, Phytochemistry 68 (2007) 1147e1155.

[13] S. Martinez-Luis, A. Perez-Vasquez, R. Mata, Natural products with calmodulin inhibitor properties, Phytochemistry 68 (2007) 1882e1903.

[14] M. Gonzalez-Andrade, M. Figueroa, R. Rodriguez-Sotres, R. Mata, A. Sosa-Peinado, An alternative assay to discover potential calmodulin inhibitors using a human fluorophore-labeled CaM protein, Anal. Biochem. 387 (2009) 64e70.

[15] G.M. Morris, D.S. Goodsell, R.S. Halliday, R. Huey, W.E. Hart, R.K. Belew, A.J. Olson, Automated docking using a Lamarckian genetic algorithm and an empirical binding free energy function, J. Comput. Chem. 19 (1998) 1639e1662.

[16] R. Huey, G.M. Morris, A.J. Olson, D.S. Goodsell, A semiempirical free energy force field with charge-based desolvation, J. Comput. Chem. 28 (2007) 1145e1152.

[17] M. Vandonselaar, R.A. Hickie, J.W. Quail, L.T. Delbaere, Trifluoperazineinduced conformational change in Ca(2þ)-calmodulin, Nat. Struct. Biol. 1 (1994) 795e801.

[18] V. Harmat, Z. Bocskei, G. Naray-Szabo, I. Bata, A.S. Csutor, I. Hermecz, P. Aranyi, B. Szabo, K. Liliom, B.G. Vertessy, J. Ovadi, A new potent calmodulin antagonist with arylalkylamine structure: crystallographic, spectroscopic and functional studies, J. Mol. Biol. 297 (2000) 747e755.

[19] Y. Hernandez-Romero, L. Acevedo, L. Sanchez Mde, W.T. Shier, H.K. Abbas, R. Mata, Phytotoxic activity of bibenzyl derivatives from the orchid Epidendrum rigidum, J. Agric. Food Chem. 53 (2005) 6276e6280.

[20] S. Suzuki, K. Ohno, T. Santa, K. Imai, Study on interactions of endocrine disruptors with estrogen receptor-beta using fluorescence polarization, Anal. Sci. 19 (2003) 1103e1108.

[21] W.J. Wedemeyer, D. Baker, Efficient minimization of angle-dependent potentials for polypeptides in internal coordinates, Proteins 53 (2003) 262e272.